ZIBELINE INTERNATIONAL™ PUBLISHING

ISSN: 2637-0778 (Online)
CODEN: ECRNAE

Environmental Contaminants Reviews (ECR)

DOI: http://doi.org/10.26480/ecr.01.2023.46.57

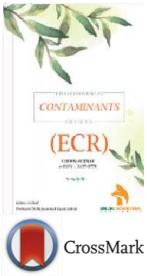

RESEARCH ARTICLE

EVALUATION OF GROUNDWATER POTENTIALITY AND QUALITY IN IKOT EKPENE-OBOT AKARA LOCAL GOVERNMENT AREAS, SOUTHERN NIGERIA

Aniekan Martin Ekanem*, Ndifreke Inyang Udosen

Geophysics Research Unit, Physics Department, Akwa Ibom State University, Nigeria
Corresponding Author Email: aniekanekanem@aksu.edu.ng, anny4mart@yahoo.com

ARTICLE DETAILS

Article History:

Received 18 August 2023
Revised 23 September 2023
Accepted 26 October 2023
Available online 06 November 2023

ABSTRACT

Adequate supply of potable water in Ikot Ekpene-Obot Akara Local Government Areas (LGAs) in Akwa Ibom State, southern Nigeria has been of a serious concern in recent times. Consequently, this study's major goal is to evaluate groundwater potentiality and quality in the LGAs via the use of the electrical resistivity technique and geochemical analysis of borehole water samples to map out the zones for the optimum location of boreholes in the area. The results of the Vertical Electrical Soundings (VES) performed at 28 locations in the area show that the lithological succession comprises sands and gravels with minor clay interbeddings at a number of locations. The main aquifer units in the area are found at depths of between 2.1 and 30.2 m, with resistivity values ranging from 40.6 to 2648.1 Ohms-metres. The generated groundwater potentiality map indicates that 89 % of the investigated area has high groundwater potential while 7 % and 4 % have low and moderate potentials respectively. The contamination level in the groundwater is shown to be very low or insignificant. Policymakers in the LGAs can use these insights to effectively manage and utilize groundwater to meet the needs of the masses.

KEYWORDS

Contamination; Geochemical; Heavy Metal; Resistivity; Aquifers

1. INTRODUCTION

Water is generally desirable for the existence of mankind. Many people around the world depend entirely on groundwater resources to satisfy their daily water demands (Reilly et al., 2008; Thomas et al., 2020; George et al., 2021; Ekanem et al., 2021, 2022a). Unfortunately, this much needed georesource may not be available in sufficient quantities in all places, or its quality may deteriorate due to a couple of factors, which include contaminations by natural or made-made activities. In recent times, there has been an intensive effort by numerous researchers in the quest for potable groundwater to meet human needs especially among urban and rural communities in developing countries (George et al., 2016, 2017; Ibuot et al., 2019; Ikpe et al., 2022; Umoh et al., 2022a; Ekanem, 2022a, b). Groundwater is contained in the pores of subsurface rock units referred to as aquifers.

One of the challenging issues in hydrology is the unequal distribution of groundwater among the pores in the aquifers (Dhinsa et al., 2022). This leads to a variation in the depth of the water table and hence, affects groundwater potential. The amount of water that can be extracted from the aquifer over time without negatively altering both the volume and the quality of the water or earth layers overlying the aquifer system is referred to here as groundwater potentiality. Additionally, water being a universal solvent can become polluted and thus unsafe for human consumption (Thomas et al., 2020; Ekanem et al., 2022a). This is particularly dependent on the make-up of the layers above the aquifer. Groundwater contamination poses a serious risk to the quality and availability of this crucial georesource and is in fact a worldwide threat (Kumar and Krishna, 2020; Ekanem et al., 2022a).

Groundwater quality in this context refers to the standard or state of water that can be drawn from the aquifer. It has to do with the suitability of groundwater for human usage. The quality of groundwater is dependent on several variables, which include temperature, acidity (pH), total dissolved solids (TDS), particulate matter (turbidity), dissolved oxygen, hardness and suspended sediments, nitrates, ions contents, etc. These factors each have unique effects on the quality and potability of groundwater. In order to safeguard human health, keep food supply secure and preserve the ecosystems, groundwater resources need to be protected.

Although superficial geological aquifer units are important groundwater reservoirs, it can be challenging, pricey and arduous to get adequate hydrogeological data to adequately define their structural spread and hydrological conditions (Obiora et al., 2016; George et al., 2018; Ekanem et al., 2020). Sufficient information on the potentiality and water quality of the hydrogeological units is paramount to efficient groundwater management. These difficulties have been overcome over time by the electrical resistivity technology, which has been successfully employed in numerous groundwater studies (Evans et al., 2015; Ibuot et al., 2019; Ekanem, 2021; Ikpe et al., 2022; Ekanem et al., 2022a, b; Ekanem, 2022a, b; Umoh et al., 2022a,b). The technology allows easy determination of the primary aquifer properties (i.e. depth, resistivity and thickness) using geological truth data as controls.

These variables are then used to calculate other aquifer secondary properties like the Dar-Zarrouk parameters (longitudinal conductance and Transverse resistance), coefficient of electrical resistivity anisotropy, transmissivity etc, which may be utilized in the characterization of the hydrogeological units in terms of protectivity, potentiality and vulnerability potentials (Ekanem et al., 2020; 2021). The transverse resistance for instance is a function of aquifer thickness and resistivity and has been shown to be proportional to groundwater potentiality (Henriet,

Quick Response Code	Access this article online	
	Website: www.contaminantsreviews.com	DOI: 10.26480/ecr.01.2023.46.57

Cite The Article: Aniekan Martin Ekanem, Ndifreke Inyang Udosen (2023). Evaluation of Groundwater Potentiality and Quality in Ikot Ekpene-Obot Akara Local Government Areas, Southern Nigeria. *Environmental Contaminants Reviews, 6(1): 46-57.*

1976; Umoh et al., 2022a; Ekanem et al., 2022b).

The rural and urban communities in the investigated area (Ikot Ekpene - Obot Akara LGAs), rely on groundwater georesource for their domestic and other uses. Over the years, the area has experienced rising solid wastes due to rapid increase in human population occasioned by the establishment of small scale industries like wood industries, palm fruit processing mills, hospitality industries, banks, construction companies, transport companies and other commercial activities (Umoh and Etim, 2013; Ekanem et al., 2022a). With increasing population and other economic activities in the area, it is expedient to carry out an evaluation of the groundwater potentiality and water quality to map out the zones that can sustain water boreholes all year round and of course, with good water quality.

The aquifer system may get contaminated by leachates created by the breakdown of solid wastes especially by rainfall or surface run-off. Research shows that majority of the exploitable aquifer units in the LGAs lack adequate pervious overlying layers and therefore have weak/poor protection to contaminants that are surface or near surface based (George 2021; Ekanem et al., 2021; Ikpe et al., 2022; Ekanem et al., 2022a; Ekanem 2022a). There is need to firm up these findings by carrying out an evaluation of the water quality indices aside evaluating the area's groundwater potentiality. Thus, the primary aim of this research work is to evaluate the groundwater potentiality and quality via a combined use of the surface electrical resistivity technology and hydrogeochemical analysis of underground water samples in the research region. This is particularly vital for the policymakers to instigate effective groundwater management plans in the research region to satisfy the water demands of the residents.

2. Site Description and Geology of The Research Area

The research area comprises Ikot Ekpene and Obot Akara LGAs in the northern segment of Akwa Ibom state, southern Nigeria as depicted in Figure 1. The area lies in the Niger Delta province approximately between latitudes 5°8′ and 5°20′ north and 7°32′ and 7°46′ east, respectively. The area has an equatorial climate with two distinctive seasons, namely the dry and the wet seasons, which begin from November till about late February and March till about late October respectively (George et al., 2016; 2017). Even so, small localized shifts in these seasons' lower and upper limits have been observed as a result of climate changes worldwide (George et al., 2018; 2021). Yearly rainfall in the area varies between 2008 and 2289 millimetres whereas the mean yearly temperature is between 20 and 35 °C respectively in the wet and dry seasons (Ekanem, 2020; Isaiah et al., 2021; Ekanem, 2021; 2022a).

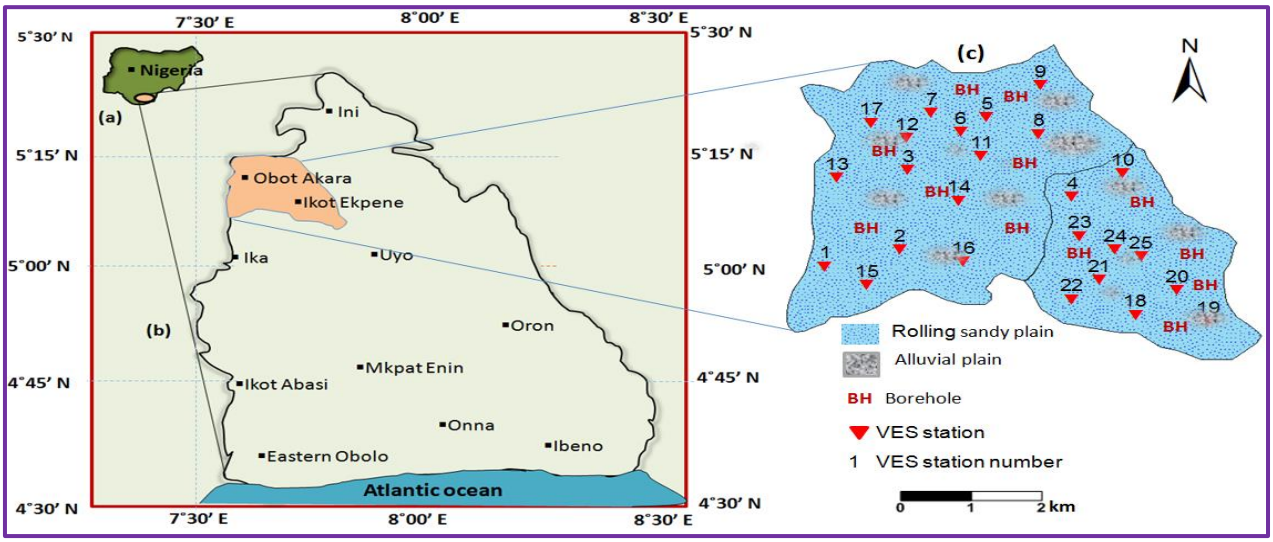

Figure 1: Schematic map of the research area (a) Nigeria showing Akwa Ibom State (b) Akwa Ibom State showing the research area (c) research area displaying its geology, sounding stations and borehole locations

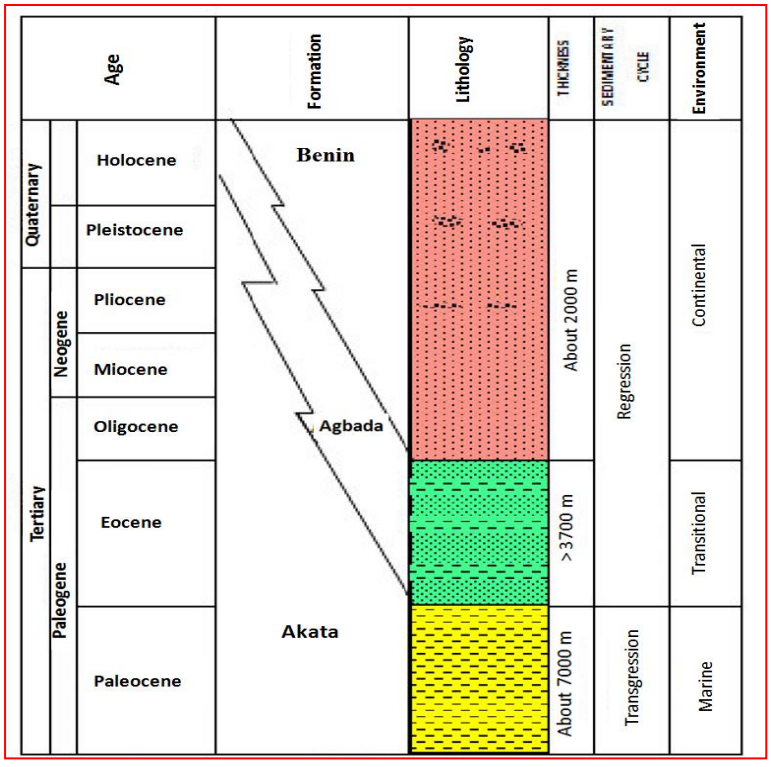

Figure 2: General Stratigraphy of the Niger Delta, where the study area is situated (adapted from Obaje, 2009)

Figure 2 depicts the broad stratigraphy of the Niger Delta. The topmost part of the Delta is the Benin Formation, also known as the Coastal Plain Sands (CPS). The sands in the Benin Formation are unevenly sorted and range in sizes from fine to coarse and gravelly (Short and Stauble 1967; Mbipom et al., 1996). Groundwater abstraction in the research area is done in the Benin Formation, which has minor clay interbeddings in some places, thus forming multi-aquifer systems at these respective places (Reijers et al., 1987; Esu et al., 1999; George et al., 2016). A key hydrocarbon bearing unit known as the Agbada Formation underlies the Benin Formation while the Akata Formation forms the bottom of the Niger Delta as illustrated in Figure 2 (Short and Stauble, 1967; Stacher, 1995).

2. MATERIALS AND METHODS

The vertical electrical sounding (VES) technique was utilized to gain insight into the electrical resistivity structure of the subsurface of the area under investigation. The technique, executed using the Schlumberger electrode arrangement allows the determination of three key subsurface layer geoelectric properties, which are thickness, resistivity and depth. The resistivity variation pattern of the identified layers was used in conjunction with borehole drilling data to define the various lithological units and their properties in the survey area. Groundwater quality indices were evaluated from the laboratory geochemical analysis of 12 borehole water samples collected in the locality of the sounding stations in the research area.

2.1 Geo-sounding Measurements and Interpretation

A total of 28 geo-sounding measurements were carried out via the use of the IGIS resistivity meter at select communities in the research area as displayed in Figure 1. The Schlumberger electrode array, which involves the use of four collinear electrodes, was employed in this research work. Two outer electrodes A and B, known as the current electrodes, were driven into the ground to put in electric current (I) into the earth layers, whereas two other inner electrodes M and N (potential electrodes) were also driven into the ground to sense the potential difference (V) developed, all in a linear arrangement.

All the electrodes were joined to the respective terminals of the measuring instrument, which indicated the apparent resistance R_a (V/1) of the earth layers through which the electric current has passed on its display unit. At each sounding locations, the electrode distance AB = a and MN = b were systematically increased about the centre from 1 to a maximum of 1000 m and 0.5 a maximum of 25 m respectively in such a manner as to fulfil the potential gradient hypothesis of AB ≥ 5 MN (George et al., 2016; Umoh et al., 2022a, b; Ekanem 2022a, b). Some of the soundings were made in the locality of drilled water boreholes, whose logged data helped in the identification and demarcation of the different litho units.

The acquired VES data were interpreted manually and with the use of the computer software program known as the WINRESIST. The manual interpretation involved the calculation of the apparent resistivity data for each sounding stations, plotting of the resistivity data on a bi-logarithmic scale and manual smoothening of the plotted curves to reveal the dominant resistivity variation pattern in the study. Equation 1 was used to calculate the apparent resistivity ρ_a for each of the sounding stations.

$$\rho_a = \pi * \left\{ \frac{\left(\frac{a}{2}\right)^2 - \left(\frac{b}{2}\right)^2}{b} \right\} * R_a \quad (1)$$

Manual smoothening was adopted to eradicate spurious signals that would have resulted in high root mean square errors (RMSE) in the computer phase of the data interpretation (Evans et al., 2015; George et al., 2020; Ekanem et al., 2022a, b). This was performed by calculating the mean of the two values of ρ_a at point of cross-over point and discarding any outliers anywhere it was indispensable in such a manner as to maintain the prevailing resistivity variation pattern in the data (Ekanem, 2021; George et al., 2020, 2022a, b)).

The computer interpretation was based on the least-square iteration algorithm, which requires initial input of the preliminary layer thicknesses and resistivities (Vander and Sporry 1993). The utilized WINRESIST software program computes a hypothetical model based on these initial input variables and matches it with the processed VES field data to produce the eventual resistivity models of the penetrated earth subsurface strata. The geological drilling data were used to refine the interpreted layers at this phase and the eventual resistivities and thicknesses obtained were considered as the true geoelectric first-order parameters of the penetrated layers. Figure 3 depicts samples of the eventual VES model curves and their correlation with the borehole lithological data.

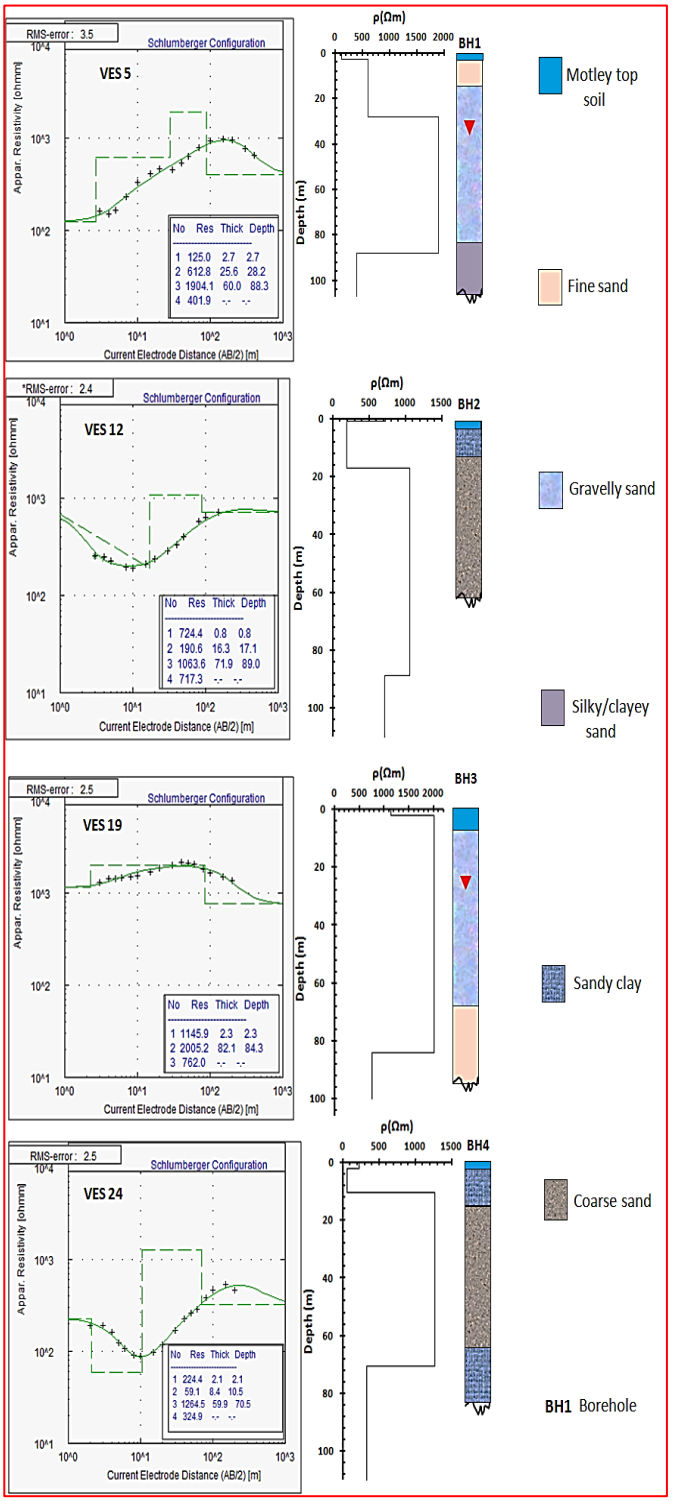

Figure 3: Sample VES curves and their correlation with borehole lithology logs

2.2 Aquifer Potentiality Evaluation

The evaluation of groundwater potentiality in this study was carried out by the combined use of the second order geoelectric variables; transverse resistance, coefficient of resistivity anisotropy and groundwater yield potential index (GWYPI). For a given layer with resistivity ρ and thickness h, the transverse resistance T is mathematically given by Equation 2.

$$T = \rho . h \quad (2)$$

For a pile of n layers, Equation 3 gives the overall transverse resistance:

$$T_t = \sum_i^n \rho_i . h_i \quad (3)$$

where ρ_i and h_i are the resistivity and thickness of the ith layer respectively. On the other hand, Equation 4 gives the vertical resistivity or transverse (ρ_v) for a pile of n-layers.

$$\rho_v = \frac{\sum_i^n h_i \rho_i}{\sum_i^n h_i} \quad (4)$$

The current flows in this case vertically through the layers. In the case of longitudinal or horizontal resistivity, current flows parallel to the layers in a horizontal direction and the longitudinal or horizontal resistivity (ρ_h) is given by Equation 5.

$$\rho_h = \frac{\sum_i^n h_i}{\sum_i^n \frac{h_i}{\rho_i}} \quad (5)$$

The resistivity coefficient of anisotropy (λ) is computed from the transverse and longitudinal resistivities through equation 6.

$$\lambda = \sqrt{\frac{\rho_v}{\rho_h}} \quad (6)$$

Finally, the groundwater potential yield index (GWPYI) is computed using Equation 7 (Olubusola et al. 2018).

$$GWYPI = \lambda \times T_t \quad (7)$$

The computed values of GWYPI can be used to grade the groundwater potentiality based on the categorization of presented in Table 1 (Olubusola et al., 2018; Umoh et al., 2022a).

Table 1: Groundwater Potentiality classification (Olubusola et al., 2018; Umoh et al., 2022a)

GWYPI	Groundwater Potentiality classification
> 30000	Very high
10000 - 30000	High
5000 - 10000	Moderate
2000 - 5000	Low
474 - 2000	Very low

2.3 Collection of Borehole Water Samples and Geochemical Analyses

Borehole water samples were collected at 12 locations near the VES stations in two 75 ml plastic bottles respectively. One bottle was used for cations while the other was used for anions in each borehole location. The bottles were rinsed thrice with the water sample at each location prior to the collection of the sample. The collected samples were sent right away to the laboratory for chemical analysis for main cations (sodium (Na), copper (Cu), iron (Fe), manganese (Mn), calcium (Ca), potassium (K), cadmium (Cd), nickel (Ni), chromium (Cr), lead (Pb) and magnesium (Mg)) and anions (bicarbonates, sulphates, chloride and sulphides).

Temperature and pH were determined directly on site by the use of a Waterproof pH/TDS/ EC/Temperature meter. Geochemical evaluation of the concentrations of the anions and cations in the collected water samples was done in the laboratory in accordance with standard procedures set out by the American Public Health Association's (APHA, 2005). In the laboratory, the concentrations of the anions were determined via the use of the Atomic Absorption Spectrophotometer (AAS) (Varian spectra 100 model) while that of the cations were obtained via titrimetric analyses (Thomas et al., 2020; George, 2021). Table 2 presents a summary of the Measured Water Sample variables in the research area.

Table 2: Summary of measured parameters from water samples in the study area

S/N	Borehole	BH 1	BH 2	BH 3	BH 4	BH 5	BH 6	BH 7	BH 8	BH 9	BH10	BH11	BH12
	Latitude (°)	5.251	5.2867	5.2733	5.2532	5.2335	5.2024	5.1981	5.2110	5.1568	5.1832	5.1680	5.1760
	Longitude (°)	7.703	7.6369	7.5984	7.5989	7.6235	7.6992	7.7117	7.6820	7.7442	7.6914	7.6690	7.7111
	Location	Iko Atasung	Ikwen	Okpo Eto	Ikot Idem Udo	Ikot Ukpong	Ikot Abia Idem	Ikono road	Uruk Uso	Utu Edem Usung	Ifuho	Ikot Osurua	Library Avenue
1	Temperature (°C)	28.20	28.40	27.30	27.10	27.20	27.60	27.30	27.10	27.30	27.20	28.10	28.30
2	pH	6.00	6.20	5.90	5.90	5.80	9.80	6.60	6.40	6.00	5.60	7.50	7.50
3	TDS (ppm)	1.00	3.00	1.00	1.00	1.00	4.50	2.00	1.00	2.00	4.00	56.00	18.90
4	Cl^- (mg/L)	1.80	1.70	2.20	3.00	3.00	3.31	2.20	1.03	1.10	1.30	12.20	8.10
5	CO_3^- (mg/L)	1.00	1.00	2.30	1.40	1.20	5.77	1.00	1.00	1.50	1.70	2.20	2.70
6	SO_4^{2-} (mg/L)	1.40	1.20	1.55	2.00	2.50	4.10	2.20	1.30	2.20	1.20	16.00	18.60
7	Na^+ (mg/L)	1.00	1.40	2.70	3.40	5.50	9.10	1.05	1.10	2.30	2.70	1.20	4.20
8	K^+ (mg/L)	0.20	0.20	0.30	1.20	0.50	1.60	0.11	0.11	0.20	0.20	0.40	0.80
9	Mg^{2+} (mg/L)	1.47	1.10	1.30	1.70	1.60	2.20	1.70	1.20	2.20	2.20	2.00	2.70
10	Ca^{2+} (mg/L)	0.06	0.05	0.07	0.04	0.07	1.70	0.05	0.05	0.07	0.05	0.08	0.08
11	Fe^{2+} (mg/L)	0.0053	0.0043	0.0048	0.0553	0.0050	0.0825	0.0550	0.0543	0.0875	0.0925	0.1000	0.1000
12	Cu^{2+}(mg/L)	0.0650	0.0703	0.1015	0.0568	0.0665	0.0825	0.0513	0.0840	0.0548	0.0488	0.0800	0.0800
13	Pb^{2+}(mg/L)	0.0003	0.0005	0.0003	0.0005	0.0005	0.0005	0.0005	0.0003	0.0005	0.0005	0.0010	0.0004
14	Cd^{2+} (mg/L)	0.0055	0.0050	0.0028	0.0310	0.0028	0.0013	0.0045	0.0045	0.0050	0.0030	0.0800	0.0500
15	Cr^{2+} (mg/L)	0.0028	0.0053	0.0035	0.0250	0.0048	0.0018	0.0288	0.0510	0.0028	0.0055	0.1200	0.1800
16	Mn^{2+} (mg/L)	0.0165	0.0100	0.0055	0.0260	0.0063	0.0060	0.0103	0.0305	0.0170	0.0333	0.0600	0.0600
17	Ni^{2+} (mg/L)	0.0235	0.0115	0.0158	0.0290	0.0188	0.0115	0.0158	0.0290	0.0188	0.0290	0.0200	0.0200
18	Zn^{2+} (mg/L)	0.0470	0.0355	0.0483	0.0503	0.0483	0.0503	0.0553	0.0415	0.0713	0.0510	0.1300	0.1000

2.4 Evaluation of Groundwater Quality Indices

Several water quality indices are available for the appraisal of groundwater quality. These indices involve the conversion and classification of the concentration data measured from the water samples into ranges to indicate the water quality grades ranging from very poor to excellent (Backman et al., 1998; Edet and Offiong, 2002; Subba Rao, 2012; Knopek and Dabrowska, 2021; Hyarat et al., 2022). The use of these indices offers a broad overview of the water quality grade and evaluates the appropriateness of groundwater for a variety of applications for the general benefit of humankind. In this study, the groundwater quality was evaluated by using three indices. These indices are the contamination index (CI) formulated (Backman et al., 1998), the heavy metal evaluation index (HMEI) and the groundwater pollution index (GPI). The combined use of these three indices gives a high degree of reliance on the inferred interpretations/ grading of the groundwater quality in the study area.

2.4.1 Contamination Index (CI)

The contamination index is computed from the sum of the contamination factors for each of the water parameters according to Equation 8.

$$CI = \sum_{i=1}^{n} CF_i \quad (8)$$

where n is the number of water parameters considered and CF_i is the contamination factor of the ith water parameter, which is given by Equation 9.

$$CF_i = \frac{C_{m,i}}{C_{perm,i}} - 1 \quad (9)$$

$C_{m,i}$ and $C_{perm,i}$ are the respective observed or measured and upper allowable concentrations of the ith water parameter. The calculation of the contamination index in Equation 8 involves the use of the water parameters whose concentrations are above the allowable or permissible limits (Backman et al., 1998; Edet and Offiong, 2002; Knopek and Dabrowska, 2021). However, in this work, all the determined concentrations of the underground water sample parameters (Table 2) were considered regardless of whether they were below or above the allowable limits for the purpose of uniformity as in (Edet and Offiong, 2002). On the basis of the computed CI values, the contamination level is categorized into low (CI < 1), moderate (CI = 1 to 3) and high (CI > 3) (Backman et al., 1998; Edet and Offiong, 2002).

2.4.2 Heavy Metal Evaluation Index (HMEI)

The heavy metal evaluation index provides an indication of the overall water quality in terms of heavy metals (Edet and Offiong 2002). The index is calculated by the use of Equation 10.

$$HMEI = \sum_{i}^{n\Sigma} \frac{H_{mea}}{H_{max}} \quad (10)$$

where H_{mea} and H_{max} are the measured and maximum permissible concentrations of the heavy metals respectively. HMEI is broken down into three classes to rate groundwater metal pollution level, viz: low (less or equal to 10), moderate (10 to 20) and high (> 20) (Edet and Offiong 2002; Rezaei et al., 2019).

2.4.3 Groundwater Pollution Index (GPI)

The groundwater pollution index was introduced by (Subba Rao, 2012). The index is computed by following five steps. The first step entails the assignment of relative weight (W_R) to the water sample parameters on the basis of their impacts on the water standard and of course human wellbeing in general on a scale of 1 to 5 as shown in Table 3. In the second step, the weight parameter (P_W) for each of the water sample parameters is computed by the use of Equation 11.

Table 3: Statistical analysis of the measured groundwater quality parameters and WHO standards

S/N	Parameters	WHO Standard (2017)	W_R	P_W	Measured in this study			
					Minimum value	Maximum Value	Mean value	Standard Deviation
1	pH	6.50-8.50	5	0.083	5.60	9.80	6.60	1.18
2	TDS (ppm)	500.00	5	0.083	1.00	56.00	7.95	15.93
3	Cl^- (mg/L)	250.00	4	0.067	1.03	12.20	3.41	3.35
4	CO_3^- (mg/L)	250.00	3	0.050	1.00	5.77	1.90	1.35
5	SO_4^{2-} (mg/L)	250.00	5	0.083	1.20	18.60	4.52	6.05
6	Na^+ (mg/L)	200.00	4	0.067	1.00	9.10	2.97	2.39
7	K^+ (mg/L)	10.00	1	0.017	0.11	1.60	0.49	0.48
8	Mg^{2+} (mg/L)	50.00	2	0.033	1.10	2.70	1.78	0.49
9	Ca^{2+} (mg/L)	75.00	2	0.033	0.04	1.70	0.20	0.47
10	Fe^{2+} (mg/L)	0.30	4	0.067	0.0043	0.1000	0.0539	0.04
11	Cu^{2+} (mg/L)	2.00	2	0.033	0.0488	0.1015	0.0701	0.02
12	Pb^{2+} (mg/L)	0.01	5	0.083	0.0003	0.0010	0.0005	0.00
13	Cd^{2+} (mg/L)	0.1	2	0.033	0.0013	0.0800	0.0163	0.02
14	Cr^{2+} (mg/L)	0.05	5	0.083	0.0018	0.1800	0.0359	0.06
15	Mn^{2+} (mg/L)	0.10	2	0.033	0.0055	0.0600	0.0234	0.02
16	Ni^{2+} (mg/L)	0.02	5	0.083	0.0115	0.0290	0.0202	0.01
17	Zn^{2+} (mg/L)	5.00	4	0.067	0.0355	0.1300	0.0607	0.03
			$\sum W_R = 60$	$\sum P_W = 1$				

$$P_W = \frac{W_R}{\sum_{i=1}^{n} W_R} \quad (11)$$

The third step involves the computation of the status of concentration (C_S) by the dividing the concentration (C_m) of each of the measured water sample parameter by the respective allowable limit (C_{perm}) according to Equation 12.

$$C_S = \frac{C_m}{C_{perm}} \quad (12)$$

The product of the values of the weight parameter and the respective contamination status is computed to yield the overall groundwater quality (OGWQ) in the fourth step. In the last step (fifth step), the groundwater pollution index is computed from the summation of all OGWQ values by the use of equation 13.

$$GPI = \sum_{i}^{n} (OGWQ)_i = \sum_{i}^{n} P_{W,i} \times C_{S,i} \quad (13)$$

Table 4 presents the rating of the water quality on the basis of the GPI classification.

Table 4: GPI classes and Groundwater Pollution classification (Subba Rao, 2011)

GPI Class	Groundwater pollution status
< 1.0	Insignificant
1.0 - 1.5	Low
1.5 – 2.0	Moderate
2.0 – 2.5	High
> 2.5	Very high

3. Results and Discussion

3.1 Resistivity Data Interpretation Results

The results of the resistivity data interpretation are presented in Table 5. Three to four layers are revealed by the results, as constrained by the geological drilling data. The first layer generally construed as the motley topsoil, is characterized by resistivity values varying between 64.6 and

1131.8 Ohm-meters and 0.6 to 24.2 meters thickness. Continuous bioturbating and other human activities occurring in this motley topsoil may possibly be responsible for the observed resistivity variation pattern in the stratum (George et al., 2016; 2017; Ekanem et al., 2020). The second identified layer with 8.4 to 83.9 m thickness and 40.6 and 2648.1 Ωm resistivity values was construed as fine/coarse/gravelly sands at a couple of places and sandy clay at the remaining places.

Table 5: Summary of VES Data Interpretation Results

VES NO.	Location	Longitude (°)	Latitude (°)	Number of layers	Bulk Resistivity (Ωm)				Thickness (m)			Depth (m)			Aquifer layer
					ρ_1	ρ_2	ρ_3	ρ_4	h_1	h_2	h_3	d_1	d_2	d_3	
1	Ubon Ukwa	7.5588	5.1918	4	1172.1	863.6	1471.2	455.7	1.7	27.7	65.7	1.7	29.4	95.1	3
2	Nto Eton 1	7.5949	5.2026	4	847.5	239.1	994.8	332.6	1.7	12.6	73.0	1.7	14.3	87.3	3
3	Ikot Idem Udo	7.5989	5.2532	3	443.1	1343.9	628.1		9.0	73.5		9.0	82.5		2
4	Mbiaso	7.6780	5.2360	4	903.5	601.3	2073.6	1421.8	1.8	14.6	80.2	1.8	16.4	96.6	3
5	Ikwen	7.6369	5.2867	4	125.0	612.8	1904.1	401.9	2.7	25.6	60.0	2.7	28.3	88.3	3
6	Nto Esu	7.6244	5.2772	4	608.2	133.3	1706.6	414.6	4.4	20.3	82.4	4.4	24.7	107.1	3
7	Ikot Okim	7.6102	5.2892	3	200.5	1397.2	2065.0		19.5	30.2		19.5	49.7		2
8	Nto Ndang 1	7.6620	5.2760	3	205.3	2083.6	904.0		10.5	81.7		10.8	92.2		2
9	Nto Ndang 2	7.6629	5.3070	3	379.7	861.4	1834.9		22.7	75.3		22.7	98.0		2
10	Ikot Atasung	7.7030	5.2510	3	65.3	1079.8	1625.6		4.5	38.6		4.5	43.1		2
11	Oku Obom	7.6345	5.2618	3	231.1	716.0	1748.9		11.2	70.2		11.2	81.4		2
12	Okpo Eto	7.5984	5.2733	4	724.4	190.6	1063.6	717.3	0.8	16.3	71.9	0.8	17.1	89.0	3
13	Ikot Essien	7.5645	5.2482	4	399.2	97.4	359.4	789.3	3.8	8.9	40.1	3.8	12.7	52.8	3
14	Ntong Uno	7.6235	5.2335	3	263.5	495.1	1427.9		12.5	89.0		12.5	101.5		3
15	Nto Eton 2	7.5790	5.1800	3	694.6	1573.9	374.0		7.0	61.0		7.0	68.0		3
16	Imama	7.6259	5.1950	3	214.1	517.8	1101.5		14.4	83.3		14.4	97.7		3
17	Nto Edino 1	7.5812	5.2831	3	400.3	1738.5	524.6		6.6	86.3		6.6	92.9		3
18	Abiakpo Edem Idim	7.7090	5.1610	4	865.7	327.2	2041.3	637.8	0.8	9.7	64.9	0.8	10.5	75.4	3
19	Utu Ikot Ekpenyong	7.7442	5.1568	3	1145.9	2005.2	762.0		2.3	82.1		2.1	84.4		2
20	Uruk Uso	7.7292	5.1767	4	630.4	148.9	2472.8	690.4	1.3	11.1	68.1	1.3	12.4	80.5	3
21	Ifuho	7.6914	5.1832	3	213.0	970.8	1493.7		2.3	70.0		2.3	72.3		2
22	Ibong Ikot Akan	7.6780	5.1710	3	228.5	2111.6	434.5		6.1	49.3		6.1	55.4		2
23	Ibong	7.6820	5.2110	3	431.9	40.6	375.5		1.4	14.6	47.5	1.4	16.0	63.5	2
24	Ikot Abia Idem	7.6992	5.2024	4	224.4	59.1	1264.5	324.9	2.1	8.4	59.9	2.1	10.5	70.4	3
25	Ikot Otu	7.7117	5.1981	3	207.4	2648.1	1506.3		4.5	80.9		4.5	85.4	85.4	2
26	Ikot Ideh	7.5669	5.2311	4	326.2	599.1	2225.2	1273.4	0.4	24.9	71.5	0.8	25.3	96.8	3
27	Nto Edino 2	7.5897	5.2433	3	185.8	1245.8	2106.5		1.6	76.2		22.7	77.8		2
28	Usaka Annang	7.5660	5.2950	4	474.9	1063.6	489.0	2658.3	0.9	29.3	55.3	0.9	30.2	85.5	3

The third detected stratum at a depth of 10.5 to 101.5 metres with resistivity values between 354.2 and 2478.6 Ωm, was construed as fine sands/coarse sands and sandy clay in a number of places and gravelly sands in the remaining places. The fourth and last layer revealed by the resistivity data interpretation results has values of resistivity varying from 75.6 to 827.9 Ωm. This layer, with an undefined depth and thickness within the confines of the maximum current electrode configuration employed was construed as fine sand in some sites and sandy clay in other sites. The noticeable variations in the values of resistivity of these layers might possibly be a result of the irregular granular sizes of the constituent sands, which characterize the Benin Formation of the Niger Delta (Stacher, 1995; Mbipom et al., 1996). These respective results show consistency with previous results obtained (George et al., 2016; 2018; 2021; 2022a, b; Ekanem et al., 2021, 2022a, b; Ikpe et al., 2022; Umoh et al., 2022 a, b).

The dwellers of the research area extract groundwater from the second and third layer as indicated in Table 5. These respective aquifer layers are unconfined in most stations occupied with the exception of VESs 2, 6, 12, 13, 20, 23 and 24. The aquifer thickness in this case varies from 30.2 in Ikot Okim community to 89.0 in Ntong Uno community, while the aquifer resistivity varies from 40.6 to 2648.1 Ωm at Ibong and Ikot Otu communities. These distributions are respectively presented in Figure 4. The aquifer units in a great number of communities in the central portion and quite a small number of communities in the southeastern part of the research area have resistivity values of less than 900 Ωm and thicknesses of greater than 65 m, as shown in Figure 4.

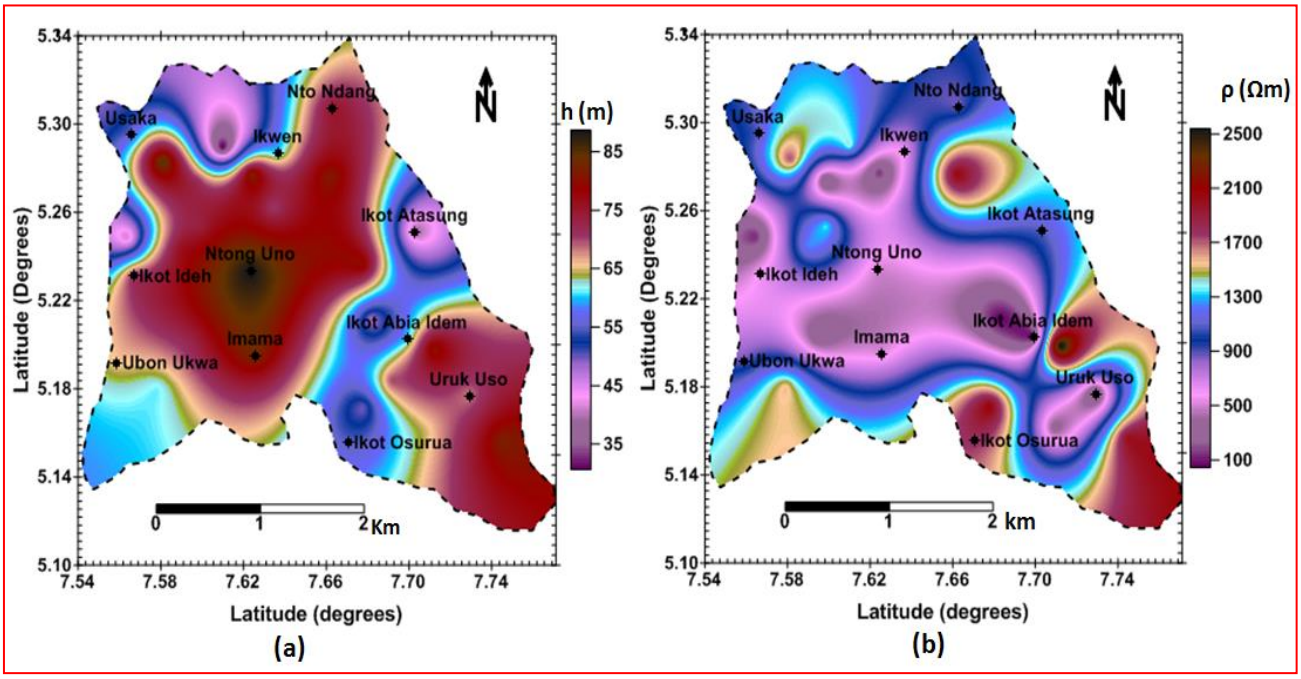

Figure 4: Distribution of (a) Aquifer thickness (b) Aquifer resistivity in the study area

3.2 Groundwater Potentiality Evaluation Results

A summary of the estimated aquifer parameters and the Groundwater Potentiality Rating (GWPR) is depicted in Table 6. The coefficient of resistivity anisotropy varies from 1.0 to 1.8 while transverse resistance of the aquifer varies between 1928.5 and 214231.3 Ωm^2. The distribution of these two parameters is illustrated in Figure 5. Values of resistivity anisotropy coefficient of 1 were obtained at VESs 1, 14, 21 and 27. This indicates that the vertical or transverse resistivity and the horizontal or longitudinal resistivity are equal. The anisotropy coefficient values are greater than 1 for all the other VES stations. This anisotropy might be possible as a result of thin bedding/claying-sand intercalations in the bedding sequence (Ekanem, 2020).

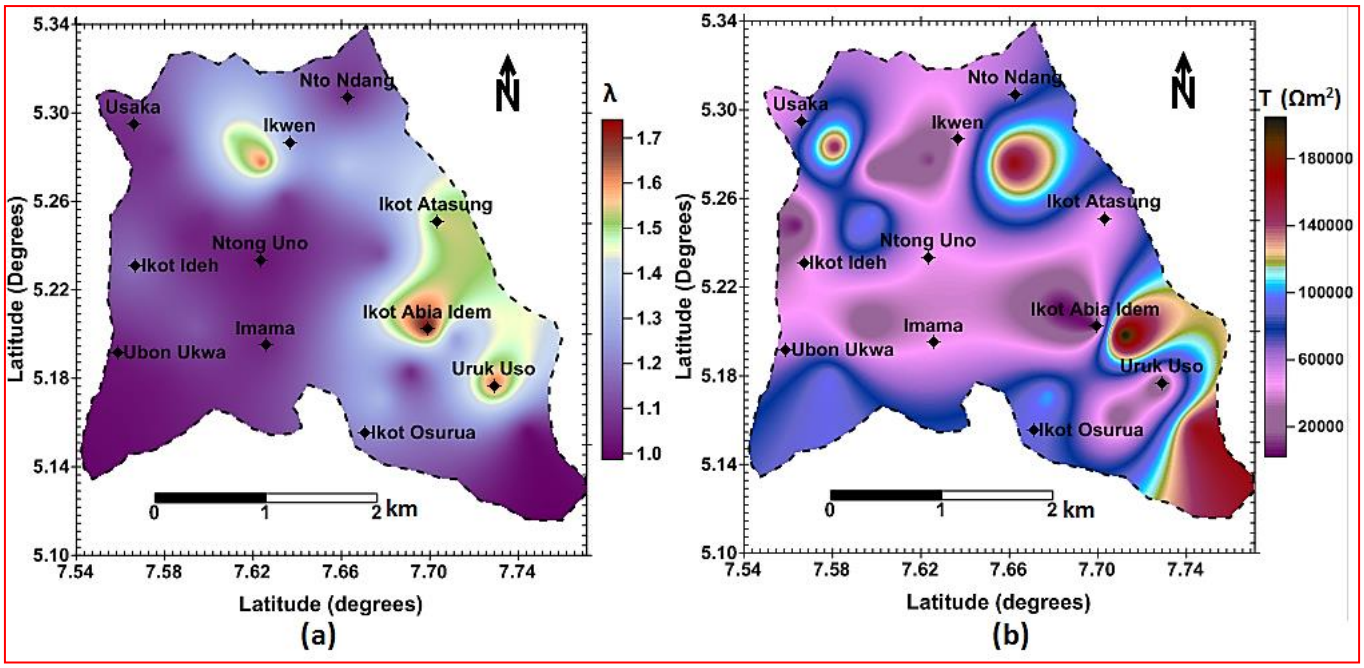

Figure 5: Distribution of (a) Resistivity anisotropy coefficient (b) Aquifer transverse resistance in the study area

Table 6: Summary of aquifer parameters and Groundwater Potentiality Rating

VES NO.	LOCATION	Aquifer Resistivity (Ωm)	Aquifer Thickness (m)	Aquifer Depth (m)	Resistivity Anisotropy coefficient (λ)	Transverse Resistance (Ωm²)	GWYPI	Groundwater Potentiality Rating
1	Ubon Ukwa	863.6	65.7	29.4	1.0	56738.5	58404.9	Very high
2	Nto Eton 1	239.1	73.0	14.3	1.1	17454.3	19865.1	High
3	Ikot Idem Udo	1343.9	73.5	9.0	1.1	98776.7	105114.2	Very high
4	Mbiaso	601.3	80.2	16.4	1.1	48224.3	53481.7	Very high
5	Ikwen	612.8	60.0	28.3	1.3	36768.0	46295.1	Very high
6	Nto Esu	133.3	82.4	24.7	1.6	10983.9	17864.1	High
7	Ikot Okim	1397.2	30.2	19.5	1.5	42195.4	62852.6	Very high
8	Nto Ndang 1	2083.6	81.7	10.8	1.4	170230.1	230427.3	Very high
9	Nto Ndang 2	861.4	75.3	22.7	1.1	64863.4	68836.7	Very high
10	Ikot Atasung	1079.8	38.6	4.5	1.5	41680.3	64096.6	Very high
11	Oku Obom	716.0	70.2	11.2	1.1	50263.2	54335.8	Very high
12	Okpo Eto	190.6	71.9	17.1	1.2	13704.1	17120.4	High
13	Ikot Essien	97.4	40.1	12.7	1.1	3905.7	4418.9	Low
14	Ntong Uno	495.1	89.0	12.5	1.0	44063.9	45031.5	Very high
15	Nto Eton 2	1573.9	61.0	7.0	1.0	96007.9	99093.4	Very high
16	Imama	517.8	83.3	14.4	1.1	43132.7	45331.5	Very high
17	Nto Edino 1	1738.5	86.3	6.6	1.1	150032.6	162273.0	Very high
18	Abiakpo Edem Idim	327.2	64.9	10.5	1.2	21235.3	25970.0	High
19	Utu Ikot Ekpenyong	2005.2	82.1	2.1	1.0	164626.9	165326.6	Very high
20	Uruk Uso	148.9	68.1	12.4	1.7	10140.1	16803.7	High
21	Ifuho	970.8	70.0	2.3	1.0	67956.0	70802.7	Very high
22	Ibong Ikot Akan	2111.6	49.3	6.1	1.3	104101.9	136533.2	Very high
23	Ibong	40.6	47.5	16.0	1.5	1928.5	2931.0	Low
24	Ikot Abia Idem	59.1	59.9	10.5	1.8	3540.1	6210.8	Moderate
25	Ikot Otu	2648.1	80.9	4.5	1.2	214231.3	265976.2	Very high
26	Ikot Ideh	599.1	71.5	25.3	1.2	42835.7	50546.6	Very high
27	Nto Edino 2	1245.8	76.2	22.7	1.0	94930.0	99462.7	Very high
28	Usaka Annang	1063.6	55.3	30.2	1.1	58817.1	62887.1	Very high
	Minimum	40.6	30.2	2.1	1.0	1928.5	2931.0	
	Maximum	2648.1	89.0	30.2	1.8	214231.3	265976.2	
	Average	920.2	67.4	14.4	1.2	63334.6	73510.5	

Figure 5b shows that transverse resistance values of less than 5000 Ωm^2 were obtained for only two VES stations (VESs 13 and 23). By implication, the high values of the transverse resistance indicate high groundwater potentiality (Henriet, 1976; Umoh et al., 2022a). The estimated values of the GWYPI range between 2931.0 to 265976.2 Ωm^2 as shown in Figure 6a. The aquifer depth, depicted in Figure 6b ranges from 2.1 to 30.2 m. Most of the aquifers occur at a depth of between 10 and 20 m, especially in the central portion of the research area. Based on the classification of the GWYPI values of Table 1, the groundwater potentiality was divided into low (7%), moderate (4%), high (18%) and very high (71%) classes respectively. These categorizations are illustrated in the groundwater potentiality rating map of Figure 7. These results shows that around 89 % of the aquifer units in the research area have the capability of sustaining water wells to meet the ever increasing needs of the inhabitants.

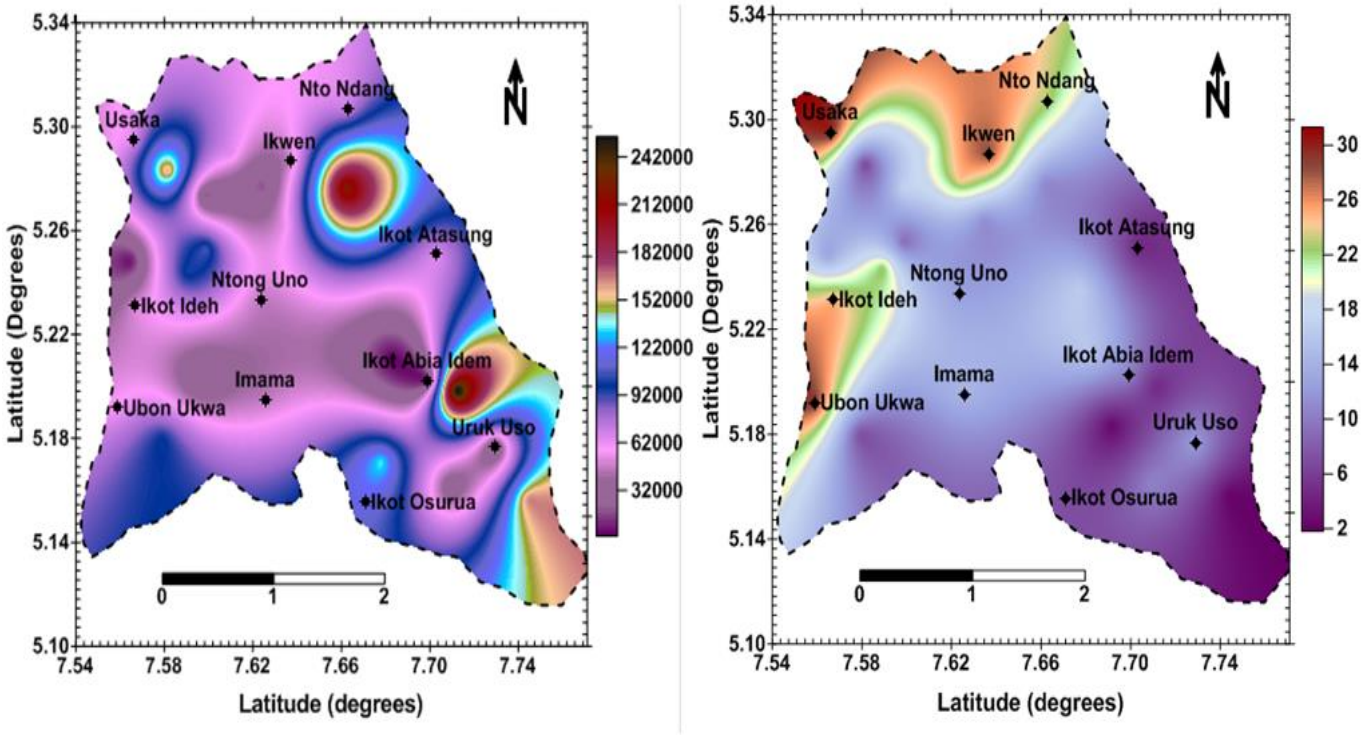

Figure 6: Distribution of (a) GWPYI (b) Aquifer Depth in the study area

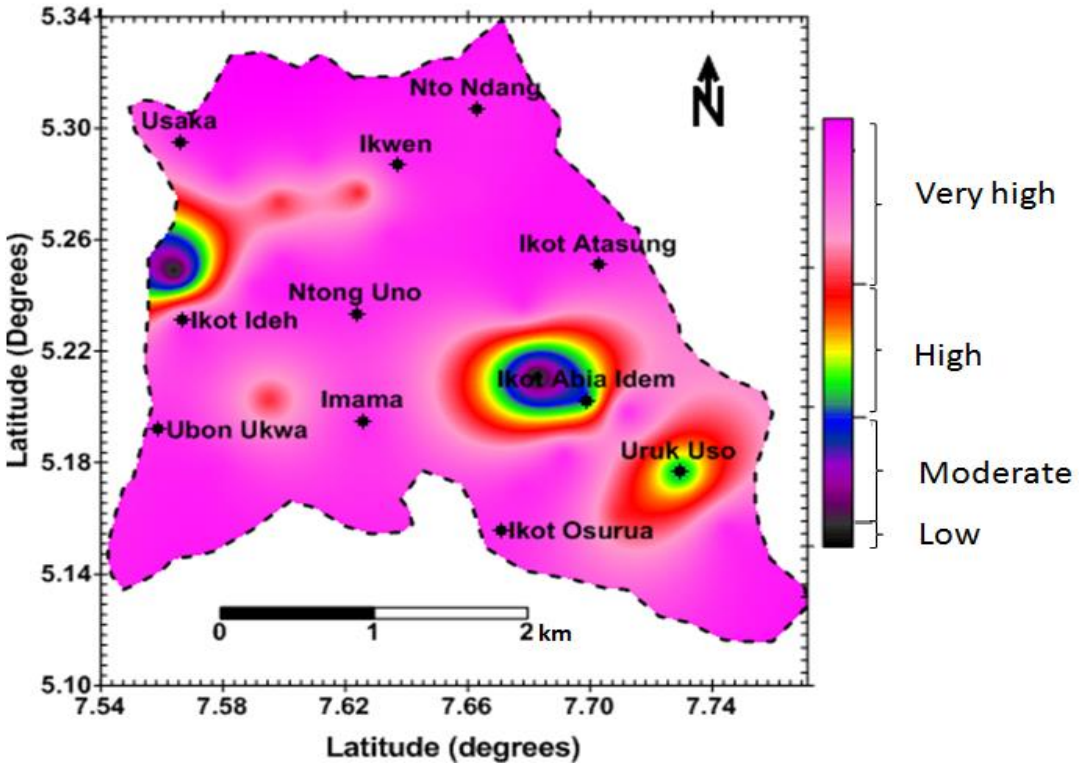

Figure 7: Groundwater potentiality map of the study area

3.3 Groundwater Quality Indices Evaluation Results

The outcomes of the statistical analysis of the measured water quality parameters and the corresponding standards of the World Health Organization (WHO) show that the values of most of the parameters are well below the standard limits with the exception of parameters like pH at some locations (boreholes 1, 2, 3, 4, 5, 6, 8, 9 and 10), chromium (boreholes 11 and 12) and nickel ions (boreholes 1, 8, 10, 11 and 12) (Tables 2 and 3). The statistical data in Table 3 show that TDS has the highest variability with a standard deviation of 15.93 while Pb^{2+} has the least variability with a standard deviation of approximately 0. Table 7 summarizes the result outcomes of the calculated groundwater quality indices.

Table 7: Summary of the computed groundwater quality indices in the study area

S/N	BOREHOLE	PIG	CI	HEI	Groundwater Contamination Status
1	1	0.18	-15.69	1.59	Low/insignificant
2	2	0.13	-16.26	0.99	Low/insignificant
3	3	0.14	-16.17	1.11	Low/insignificant
4	4	0.26	-14.31	2.96	Low/insignificant
5	5	0.16	-15.95	1.34	Low/insignificant
6	6	0.19	-15.37	1.33	Low/insignificant
7	7	0.20	-15.37	1.83	Low/insignificant
8	8	0.30	-14.11	3.12	Low/insignificant
9	9	0.18	-15.60	1.67	Low/insignificant
10	10	0.23	-14.92	2.39	Low/insignificant
11	11	0.46	-11.50	5.39	Low/insignificant
12	12	0.54	-10.67	6.29	Low/insignificant
	Minimum value	0.13	-16.26	0.99	
	Maximum value	0.54	-10.67	6.29	

The values of the contaminated index are all less than 1, ranging from -16.26 to -10.27. This indicates very low/insignificant contamination level of groundwater. The heavy metal evaluation index varies from 0.99 to 6.29. This index was only computed for the heavy metals determined from the geochemical analysis of the groundwater samples. These metals are sodium, potassium, magnesium, calcium, iron, copper, lead, cadmium, chromium, manganese, nickel and zinc. According to a study, heavy metal pollution is thought to be more hazardous than other types of water pollution due to their high level of toxicity (Tian et al., 2019). The computed values of the HMEI in this study are all below 10, implying that the groundwater metal pollution level is very low or insignificant (Edet and Offiong, 2002; Rezaei et al., 2019). The values of the computed groundwater pollution index vary from 0.13 to 0.54, which are again less than 1.

On the whole, the results of the three water quality indices reveal that the contamination level of the groundwater in the study area is very low or insignificant according to the data in Table 4. By implication, the groundwater quality of the analysed groundwater samples is adjudged to be very good. The combined use of the three indices gives therefore provides a high degree of reliance on the inferred interpretations/ grading of the groundwater quality in the study area.

4. Conclusion

The evaluation of groundwater potentiality and quality indices has been carried out in this study via the use of electrical resistivity technique and hydrogeochemical analyses of groundwater samples. Georesistivity soundings were made at twenty eight locations in the study area. The results of the data interpretation show that the area is made up of three to four layers whose lithological succession comprises sands and gravels with minor clay interbeddings at a number of locations. The economically exploited aquifer units in the area are found at depths of between 2.1 and 30.2 m in the second layer at a few locations and in the third layer at other locations, respectively with resistivity values ranging from 40.6 and 2648.1 Ohms-metres. The estimated groundwater yield potential index (GWYPI) ranges between 2931.0 to 265976.2 Ωm^2. On the other hand, the estimated quality indices (contamination factor, heavy metal evaluation index and groundwater pollution index) range from -16.26 to -10.27, 0.99 to 6.29 and 0.13 to 0.54 respectively.

The generated groundwater potentiality map indicates that 89 % of the investigated area has high groundwater potential while 7 % and 4 % have low and moderate potentials respectively. The three quality indices all show that the contamination levels in the groundwater are very low or insignificant. By implication, the aquifer units in the area have the capacity of sustaining water wells all year round and the groundwater quality is generally good for human consumption and other uses. Although these findings are particularly vital for policymakers to instigate efficient groundwater management and utilization plans in the research area to meet the water demands of the people, further studies involving microbiological analyses of groundwater samples is recommended in the area to validate the results of this study. Most specifically, such studies should include analysis of parameters like Nitrates, Phosphates, Ammonia and Escherichia Coli in order to offer more information regarding groundwater susceptibility to domestic wastewater contamination.

Acknowledgements

The authors wish to thank the Tertiary Education Trust Fund (TETFund), Nigeria for providing financial support for this work and permitting the authors to publish the results. The authors are also appreciative of the supports from all the GRG members of Physics Department in Akwa Ibom State University.

References

Backman, B., Bodis, D., Lahermo, P., Rapant, P., Tarvainen, T., 1998. Application of a groundwater contamination index in Finland and Slovakia. Environmental Geology, 36 (1-2), Pp. 55 – 64.

Dhinsa, D, Tamiru, F., Tadesa, B., 2022. Groundwater potential zonation using VES and GIS techniques: A case study of Weserbi Guto catchment in Sululta, Oromia, Ethiopia. Heliyon 8. https://doi.org/10.1016/j.heliyon.2022.e10245

Edet, A.E., Offiong, O.E., 2002. Evaluation of water quality pollution indices for heavy metal contamination monitoring, a study case from Akpabuyo-Odukpani area, Lower Cross-River Basin (Southeastern Nigeria). Geojournal, 57, Pp. 295 – 304.

Ekanem, A.M., 2020. Georesistivity modelling and appraisal of soil water retention capacity in Akwa Ibom State University main campus and its environs, Southern Nigeria. Model. Earth Syst. Environ. 6, Pp. 2597–2608. https://doi.org/10.1007/s40808-020-00850-6

Ekanem, A.M., 2022a. AVI- and GOD-based vulnerability assessment of aquifer units: a case study of parts of Akwa Ibom State, Southern Niger Delta, Nigeria. Sustain. Water Resour. Manag. 8, Pp. 29. https://doi.org/10.1007/s40899-022-00628-x

Ekanem, A.M., 2022b. Georesistivity Modelling and Mapping of Aquifer Geometry and Hydraulic Characteristics in a Sedimentary Environment. Water Conservation Science and Engineering, 7 (4), Pp. 585-598

Ekanem, A.M., Akpan, A.E., George, N.J., Thomas, J.E., 2021. Appraisal of protectivity and corrosivity of surficial hydrogeological units via geo-sounding measurements. Environ Monit Assess, 193, Pp. 718. https://doi.org/10.1007/s10661-021-09518-9.

Ekanem, A.M., George, N.J., Thomas, J.E., Nathaniel, E.U., 2020. Empirical Relations Between Aquifer Geohydraulic–Geoelectric Properties Derived from Surficial Resistivity Measurements in Parts of Akwa Ibom State, Southern Nigeria. Natural Resources Research, 29 (4), Pp. 2635-2646. https://doi.org/10.1007/s11053-019-09606-1.

Ekanem, A.M., Ikpe, E.O., George, N.J., Thomas, J.E., 2022a. Integrating geoelectrical and geological techniques in GIS-based DRASTIC model of groundwater vulnerability potential in the raffia city of Ikot Ekpene and its environs, southern Nigeria. International Journal of Energy and Water Resources. https://doi.org/10.1007/s42108-022-00202-3

Ekanem, A., 2021. Estimation of aquifer geohydrodynamic properties using the Inverse Slope method. Researchers Journal of Science and Technology, 1 (1), Pp. 1-16.

Ekanem, K.R., George, N.J., and Ekanem, A.M., 2022b. Parametric characterization, protectivity and potentiality of shallow hydrogeological units of a medium-sized housing estate, Shelter Afrique, Akwa Ibom State, Southern Nigeria. Acta Geophysica., 70 (2), Pp. 879 - 895

Esu, E.O., Okereke, C.S., Edet, A.E., 1999. A regional hydrostratigraphic study of Akwa Ibom State southeastern Nigeria. Global Journal of Pure and Applied Sciences, 5 **(**1), Pp. 89-96.

Evans, U.F., George, N.J., Ekanem, A.M., 2015. Analysis of Microstructural Properties of Paleozoic Aquifer in the Benin Formation, using Grain Size Distribution Data from Water Borehole in Akwa Ibom State, Nigeria. IOSR Journal of Applied Geology and Geophysics 3 (4), Pp. 25-30. (DOI: 10.9790/0990-03422530)

George, N.J., 2021. Geo-electrically and hydro geologically derived vulnerability assessments of aquifer resources in the hinterland of parts of Akwa Ibom State, Nigeria. Solid Earth Sciences, 6 (2), Pp. 70 – 79.

George, N.J., Bassey, N.E., Ekanem, A.M., Thomas, J.E., 2020. Effects of anisotropic changes on the conductivity of sedimentary aquifers, southeastern Niger Delta, Nigeria. Acta Geophysica, 68 (6), Pp. 1833-1843.

George, N.J., Ekanem, A.M., Thomas, J.E., and Ekong, S.A., 2021. Mapping depths of groundwater-level architecture: implications on modest groundwater-level declines and failures of boreholes in sedimentary environs. Acta Geophysica, 69, Pp. 1919–1932. https://doi.org/10.1007/s11600-021-00663-w

George, N.J., Ekanem, A.M., Thomas, J.E., Harry, T.A., 2022a. Modelling the effect of geo-matrix conduction on the bulk and pore water resistivity in hydrogeological sedimentary beddings. Modeling Earth Systems and Environment, 8 (1), Pp. 1335-1349.

George, N.J., Ibuot, J.C., Ekanem, A.M., George, A.M., 2018. Estimating the indices of inter-transmissibility magnitude of active surficial hydrogeologic units in Itu, Akwa Ibom State, southern Nigeria. Arab J. Geosciences, 11, Pp. 134. https://doi.org/10.1007/s12517-018-3475-9

George, N.J., Obiora, D.N., Ekanem, A.M., Akpan, A.E., 2016. Approximate relationship between frequency-dependent skin depth resolved from geoelectromagnetic pedotransfer function and depth of investigation resolved from geoelectrical measurements: A case study of coastal formation, southern Nigeria. J. Earth Syst. Sci., 125, Pp. 1379–1390. https://doi.org/10.1007/s12040-016-0744-4

George, N.J., Umoh, J.A., Ekanem, A.M., Agbasi, O.E., Jamal, A., Thomas, J.E., 2022b. Geophysical-laboratory data integration for estimation of groundwater volumetric reserve of a coastal hinterland through optimized interpolation of interconnected geo-pore architecture. Journal of Coastal Conservation, 26 (6), Pp. 56. https://doi.org/10.1007/s11852-022-00902-2

George, N.J., Ekanem, A.M., Ibanga, J.I., Udosen, N.I., 2017. Hydrodynamic Implications of Aquifer Quality Index (AQI) and Flow Zone Indicator (FZI) in groundwater abstraction: a case study of coastal hydro-lithofacies in South-eastern Nigeria. J. Coast. Conserv. 21, Pp. 759 – 776. https://doi.org/10.1007/s11852-017-0535-3

Henriet, J.P., 1976. Direct Application of the Dar Zarrouk Parameters in Groundwater Surveys. Geophysical Prospecting, 2, Pp. 344 - 353. http://dx.doi.org/10.1111/j.1365-478.1976.tb00931.x

Hyarat, T., Kuisi, M.A., Saffarini, G., 2022. Assessment of groundwater quality using water quality index (WQI) and multivariate statistical analysis in Amman-Zarqa area/ Jordan. Water Practice and Technology, 17 (8), Pp. 1582–1602. https://doi.org/10.2166/wpt.2022.076

Ibuot, J.C., George, N.J., Okwesili, A.N., Obiora, D.N., 2019. Investigation of litho-textural characteristics of aquifer in Nkanu West Local Government Area of Enugu state, southeastern Nigeria. Journal of African Earth Sciences, 153, Pp. 197-207. https://doi.org/10.1016/j.jafrearsci.2019.03.004.

Ikpe, E.O., Ekanem, A.M., George, N.J., 2022. Modelling and assessing the protectivity of hydrogeological units using primary and secondary geoelectric indices: a case study of Ikot Ekpene Urban and its environs, southern Nigeria. Model. Earth Syst. Environ. https://doi.org/10.1007/s40808-022-01366-x

Isaiah, A.I., Yamusa, A.M., Odunze, A.C., 2021. Advanced Study on Variability in Length of Rainy Season for Selected Crops Production in Coastal and Upland Areas of Akwa Ibom State, Nigeria. Cutting-edge Research in Agricultural Sciences, 6 (5), Pp. 101 - 109. https://doi.org/10.9734/bpi/cras/v6/2424E

Knopek, T., Dabrowska, D., 2021. The Use of the Contamination Index and the LWPI Index to Assess the Quality of Groundwater in the Area of a Municipal Waste Landfill. Toxics, 9 (3), Pp. 66. https://doi.org/10.3390/toxics9030066.

Kumar, A., Krishna, A.P., 2020. Groundwater vulnerability and contamination risk assessment using GIS-based modified *DRASTIC*-LU model in hard rock aquifer system in India. Geocarto International, 35 (11), Pp. 1149 - 1178. DOI: 10.1080/ 10106049.2018.1557259.

Mbipom, E.W., Okwueze, E.E., Onwuegbeche, A.A.A., 1996. Estimation of transmissivity using VES data from Mbaise area of Nigeria. Nigerian Journal of Physics, 85, Pp. 28 – 32.

Obaje, N.G., 2009. Geology and Mineral Resources of Nigeria. London: Springer Dordrecht Heidelberg, Pp. 5-14.

Obiora, D.N., Ibuot, J.C., George, N.J., Offiah, S.U., 2016. Delineation of groundwater saturation indicators and their distributions in the complex argillaceous geological units of Ezza north local government area of Ebonyi state, Nigeria. Current Science, 110 (4), Pp. 701 – 708.

Olubusola, I.S., Daniel, A.A., Oladimeji, O.K., 2018. Modeling of Groundwater Yield Using GIS and Electrical Resistivity Method in a Basement Complex Terrain, Southwestern Nigeria. Journal of Geography, Environment and Earth Science International, 16 (1), Pp. 1-17. DOI**:** 10.9734/JGEESI/2018/42102

Reijers, T.J.A., Petters, S.W., 1987. Depositional environments and diagenesis of Albian Carbonates on the Calabar Flank, SE Nigeria. Journal of Petroleum Geology**,** 10 (3), Pp. 283-294.

Reilly, T., Dennehy, K.F., Alley, W.M., Cunningham, W.L., 2008. Groundwater availability in the United State. US Geological Society Circular, 1323, Pp. 70.

Rezaei, A., Hassani, H., Hassani, S., Jabbari, N., Mousavi, S.B.F., Rezaei, S., 2019. Evaluation of groundwater quality and heavy metal pollution indices in Bazman basin, southeastern Iran. Groundw. Sustain. Dev., 9, Pp. 100245.

Short, K.C., Stauble, A.J., 1967. Outline Geology of the Niger Delta. AAPG Bull, 51, Pp. 761-779.

Stacher, P., 1995. Present Understanding of the Niger Delta hydrocarbon habitat, In, M. N Oti and G. Postma (eds.), Geology of Deltas: Rotterdam, A.A. Balkema, Pp. 257-267.

Subba, R.N., 2012. PIG: a numerical index for dissemination of groundwater contamination zones. Hydrol. Process, 26, Pp. 3344 – 3350.

Thomas, J.E., George, N.J., Ekanem, A.M., Nsikak, E.E., 2020. Electro stratigraphy and hydro geochemistry of hyporheic zone and water-bearing caches in the littoral shorefront of Akwa Ibom State University, Southern Nigeria. Environ. Monit. Assess., 192, Pp. 505. https://doi.org/10.1007/s10661-020-08436-6

Tian, M., Fang, L., Yan, X., Xiao, W., Row, K.H., 2019. Determination of Heavy Metal Ions and Organic Pollutants in Water Samples Using Ionic Liquids and Ionic Liquid-Modified Sorbents. Journal of Analytical Methods in Chemistry, Pp. 1948965. https://doi.org/10.1155/2019-/1948965

Umoh, J.A., George, N.J., Ekanem, A.M., Thomas, J.E., Emah, J.B., 2022a. Approximate delineation of groundwater yield capacity and vulnerability via secondary geo-electric indices and rock-water interaction hydrodynamic coefficients in a coastal environment. Researchers Journal of Science and Technology, 2 (3), Pp. 28 – 54.

Umoh, J.A., George, N.J., Ekanem, A.M., Emah, J.B., 2022b. Characterization of hydro-sand beds and their hydraulic flow units by integrating surface measurements and ground truth data in parts of the shorefront of Akwa Ibom State, Southern Nigeria. Int. J. Energy Water Resources. https://doi.org/10.1007/s42108-022-00215-y

Umoh, S.D., Etim, E.E., 2013. Determination of heavy metal contents from dumpsites within Ikot Ekpene, Akwa Ibom State, Nigeria Using Atomic Absorption Spectrophotometer. Int. J. Eng. Sci. (*IJES*), 2 (2), Pp. 123 - 129.

Vander, V.B.P.A., and Sporry, R.J., 1993. Resist: a computer program to process resistivity sounding data on PC compatibles. Computers and geosciences, 19 (5), Pp. 691-703.

WHO, 2017. Guideline for drinking water quality, 4th edition. World Health Organization, Geneva.